DOI: 10.15669/pnst.8.257

Progress in Nuclear Science and Technology
Volume 8 (2025) pp. 257-261

ARTICLE

Study on Oxygen Partial Pressure Dependence and Kinetic of Oxidation and Vaporization Behavior of Insoluble Residues (Noble Metal Precipitation) in High-Level Waste

Yuki OIWA [1*], Isamu SATO [1], Haruaki MATSUURA [1], Koya YAMAZAKI [1], Naoki TARUMI [1**], Hiroki IZUMI [3] and Haruka TADA [3]

[1] *Tokyo City University, 1-28-1, Tamazutsumi, Setagaya-ku, Tokyo 158-8557, JAPAN*
[3] *IHI Corporation, Toyosu IHI Bldg., 1-1, Toyosu 3-chome, Koto-ku, Tokyo 135-8710, JAPAN*

Noble metal precipitates (Mo, Ru, Rh, Pd, and Tc) contained in high-level radioactive liquid waste can affect the vitrification process in various ways, such as formation of yellow phase and deposition at the bottom of the glass melter. Therefore, in this study, thermogravimetric analysis was conducted to investigate the composition and oxygen partial pressure dependence of reactions such as oxidation and evaporation of alloying elements by weight change during heating.

KEYWORDS: noble metal precipitate, glass melter, vitrification, oxygen partial pressure, kinetic studies

I. Introduction

Spent nuclear fuels are reprocessed and some of them are vitrified as high-level radioactive waste for geological disposal. In the reprocessing dissolution process, the insoluble residue, which is the residue from dissolving the spent fuel, contains alloys of noble metal precipitates (Mo, Ru, Rh, Pd, and Tc).[1)] Noble metal elements are considered to have various effects on the vitrification process, such as migrating into the off-gas and blocking drain nozzles.[2)]

In a previous study, we prepared samples simulating the compositions of noble metal alloys in the insoluble residue, compared various behaviors using thermogravimetric analysis, observed the evaporation of Mo after oxide formation, and observed the formation of RuO_2. [3)] In addition, when simulated liquid waste components, glass, and alloys coexisted and were heated, it was observed that the various behaviors of Mo, Ru, and Rh (oxidation and migration to glass) depended on the alloy composition.[4)] Furthermore, since the oxygen partial pressure in the glass melter is non-uniform,[5)] the oxidation and evaporation behavior of noble metal alloys is considered to depend on the oxygen partial pressure.

To understand the behavior of noble metal alloys in more detail, this study investigated the dependence of reaction rates on composition and oxygen partial pressure in various behaviors such as oxidation and evaporation of simulated noble metal alloys by thermogravimetric analysis under simulated oxygen partial pressure similar to those in an actual glass melter.

II. Experimental Method

1. Preparation of Samples

The two composition sets (R6-2 and R6-3) to simulate the compositions of noble metal alloys generated during reprocessing for current fuels and for MOX (or high burnup) fuels handled in the future,[5,6] are prepared. In addition, a composition (R6-1) was set assuming composition changes due to nitric acid (Mo concentration is decreased due to incongruent dissolution of Mo) (**Table 1**). The numbering was arranged in order of Mo concentration.

Four of the five elements in noble metal precipitates, Mo, Ru, Rh, and Pd were used as evaluation targets. Tc, the fifth noble metal precipitate, was excluded since there are no stable isotopes of Tc. Although Re has the potential to simulate the chemical properties of Tc in aqueous solution,[6)] there are few reports of thermodynamic data and phenomena such as noble metal precipitates in solid solution, etc. In previous studies, evaluations using four elements, excluding Tc, was often sufficient to understand alloy behavior. [3,4,7)] Then powders of Mo, Ru, Rh, and Pd (Nilaco Corporation: 99.9% purity) were each weighed, placed in a moisture-proof container, and shaken to mix uniformly.

Next, the powder mixture was pressed at about 5.9 MPa using a die (Φ8 mm) to get a compact, melted in an Ar atmosphere (introduced after vacuum operation (5×10^{-3} Pa)) using an arc melting device (Techno Search Corp., TMA1-6N), and quenched with a copper hearth to obtain about 1.3 to 1.4 g of the simulated noble metal alloy. The sample surfaces were polished with water-resistant abrasive paper (#600,

*Corresponding author, E-mail: youy1916006@gmail.com

**Currently affiliated with Central Research Institute of Electric Power Industry (tarumi40522@criepi.denken.or.jp)

© Atomic Energy Society of Japan

#1000, #1500, #2000, #3000) and mirror polished with diamond paste (#1800, #3000, #8000), then subjected to SEM-EDS (Hitachi, 28TM3000) and XRD (Bruker AXS, MXP3TAHF22) to characterize the samples (surface condition, crystal structure, composition, etc.).

After that, these samples were crushed by 100 or 200 blows in a dancing mill (crucible and striking rod were tungsten carbide chrome steel (Ito Mfg. Co., Ltd., ADA-48)). Then, the samples were ground to powder using a planetary ball mill (Fritsch, P-7 Classic Line) with 10 mm diameter tungsten carbide balls in a tungsten carbide grinding vessel at 300 rpm for 10 min. The ground samples were sieved and those powdered with a maximum particle diameter of less than 50 μm were used for thermogravimetric analysis.

Table 1 Composition of powder alloy samples

	Mo [wt.%]	Ru [wt.%]	Rh [wt.%]	Pd [wt.%]
R6-1	9.3	64.6	19.1	7.1
R6-2	15.2	55.4	19.1	10.4
R6-3	21.0	59.8	13.6	5.7

2. Thermogravimetric Analysis and Observation of Samples After Heating

Temperature rise and isothermal thermogravimetric analysis were performed using a TG-DTA apparatus (Advance Science and Engineering, TGD-9500). First, the sample was stored in an alumina cell (sample housing dimensions: height 7 mm × inner diameter φ5 mm), which was placed in the beam section at the top of the TG-DTA apparatus. To simulate the oxygen partial pressure conditions at the bottom of the glass melter, argon (Ar) gas and dry air were mixed. The ratio of oxygen to Ar was adjusted at a total pressure of 1 atm to control the oxygen partial pressure to approximately 0.2, 0.07, 0.05 and 0.01 atm. The thermogravimetric analysis was performed at a heating rate of 5 K/min and held at 1173 K for 2 hours. The oxygen partial pressure conditions were set with reference to the value of oxygen partial pressure in the glass melter obtained by Sugawara et al[5] through thermodynamic equilibrium calculations.

X-ray diffraction of the heated samples was performed by XRD using Cu as the X-ray target, a scanning angle of 30 ° to 90 °, a scanning speed of 1 °/min, an acceleration voltage of 40 kV, and a tube current of 30 mA. A powdered sample after heating was embedded in resin, polished to expose the sample cross section, and the elemental distributions were observed by SEM-EDS to identify those compositions.

III. Results and Discussion

1. Thermogravimetric Analysis

Thermogravimetric analysis was performed on R6-1, R6-2 and R6-3 powder alloy samples, and weight changes were evaluated using thermogravimetric curves.

Figure 1 shows the test results of R6-1. The weight gain started around 870 K. A rapid weight gain was observed at the highest oxygen partial pressure, while the weight changes were small at low oxygen partial pressures. There was almost no weight change for the temperature plateau under all oxygen partial pressure conditions.

Figure 2 shows the test results of R6-2. The weight gain was slow for the temperature plateau, reaching 1173 K, and the weight went from increasing to decreasing at lower oxygen partial pressures.

Figure 3 shows the test results for R6-3. When the oxygen partial pressure was high, the weight showed a rapid increase in the vicinity of 970 K to 1173 K, followed by an immediate decrease. The weight changed at the temperature plateau became an increase at relatively high oxygen partial pressures but tended to decrease at the lowest oxygen partial pressures.

Based on previous studies,[3,4] we believe that this weight change is caused by the oxidation and evaporation properties in the constituent elements of the noble metal alloys. The ease of oxidation is Mo > Ru > Rh > Pd based on their Gibbs free energy. Since the weight loss of R6-3 at around 1070 K is consistent with the melting point of MoO_3 (1068 K), we assume that MoO_3 melts, quickly evaporates, and migrates. It has also been observed that Ru and Rh are oxidized depending on the oxygen partial pressure, temperature, and composition. When considering reaction kinetics, it is necessary to add oxygen partial pressure dependence, phase change, and geometry factors in addition to the above basic behaviors.

The behaviors of each element in the weight change upon heating obtained here are considered from the metallurgical observations given below.

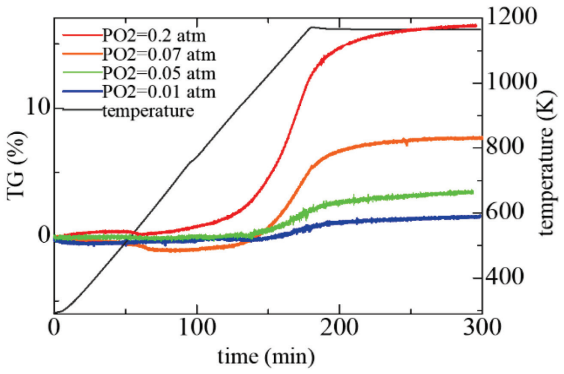

Fig. 1 Thermogravimetric analysis results for R6-1

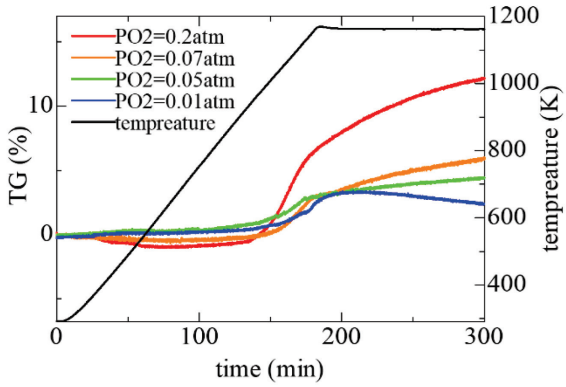

Fig. 2 Thermogravimetric analysis results for R6-2

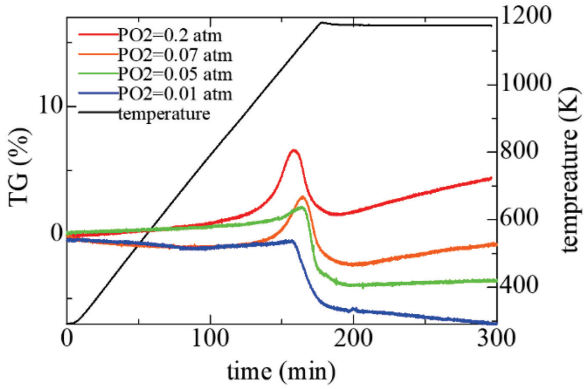

Fig. 3 Thermogravimetric analysis results for R6-3

2. Observation After Heating

(1) XRD

Figure 4 shows XRD measurement results for the samples after thermogravimetric analyses. The sample before heating showed a hexagonal close-packed (HCP) structure similar to Ru metal [8]. In cases of high oxygen partial pressure, RuO_2 peaks were observed, and no MoO_3 peaks were present (they had migrated by evaporation). This suggests that Ru mainly forms an oxide film on the large surface area of the sample or that the oxide is dispersed. It is possible that this Ru oxide acts to control the reaction rate. We also observed a peak of Pd, which is considered to have precipitated as a separate phase. This implies that the reactions are accompanied by phase changes.

When the oxygen partial pressure was low, the peak pattern due to the HCP structure before the test was observed without the formation of Ru oxide.

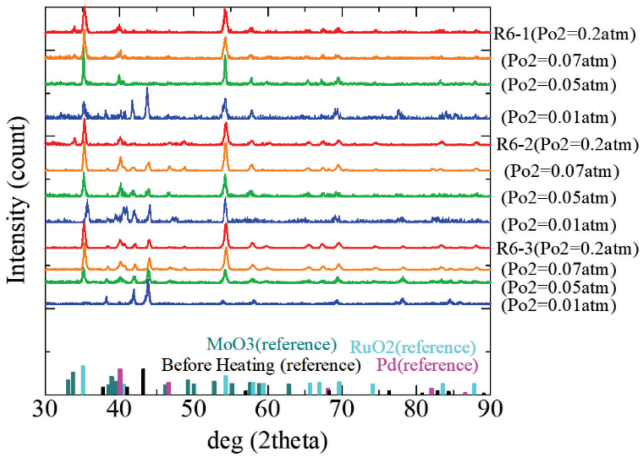

Fig. 4 XRD peak pattern after heating [8]

(2) SEM-EDS

Elemental distributions (Mo, Ru, Rh, Pd, O) and compositions were obtained from SEM-EDS for each powder sample after heating. Here, the composition was evaluated on average over an area of about 20 μm × 20 μm, where the composition can be considered a homogeneous phase.

Figures 5 to **9** show SEM images and EDS mapping results.As to R6-2 (Mo, 15.2 wt.%), Mo rich and Mo poor phases were separated at relatively high oxygen partial pressures (**Table 2**), and the Mo poor phase was porous in the SEM image. When the oxygen partial pressure was high, the XRD peak pattern of R6-2 (Fig. 4) strongly captured peaks that appeared to be RuO_2, but the SEM-EDS did not clearly indicate areas that were oxide layers with high Ru content. This implies that RuO_2 may be an oxide film of less than μm order in thickness at the interface between the poor and rich phases, or only a part of the Ru is oxidized and dispersed in the poor phase.

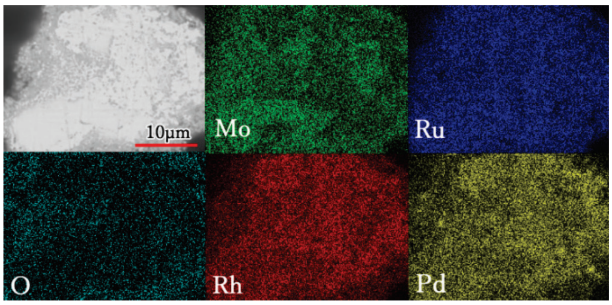

Fig. 5 EDS mapping of R6-2 (P_{O2}=0.2 atm) after heating

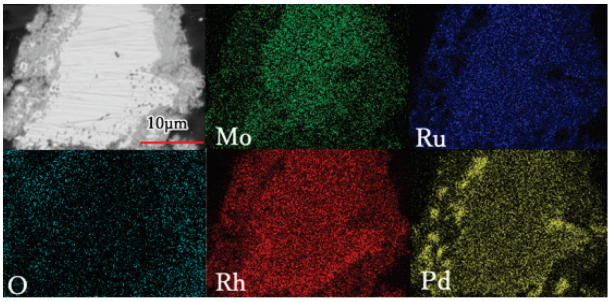

Fig. 6 EDS mapping of R6-2 (P_{O2}=0.07 atm) after heating

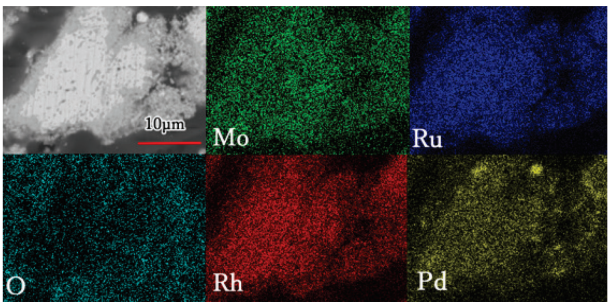

Fig. 7 EDS mapping of R6-3 (P_{O2}=0.2 atm) after heating

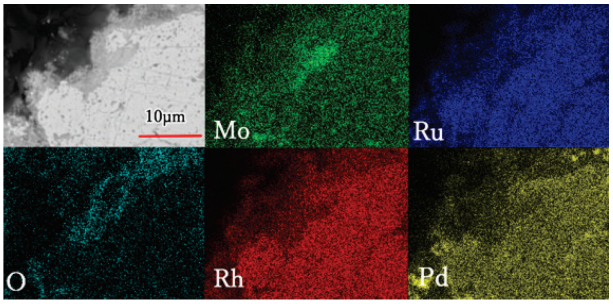

Fig. 8 EDS mapping of R6-3 (P_{O2}=0.05 atm) after heating

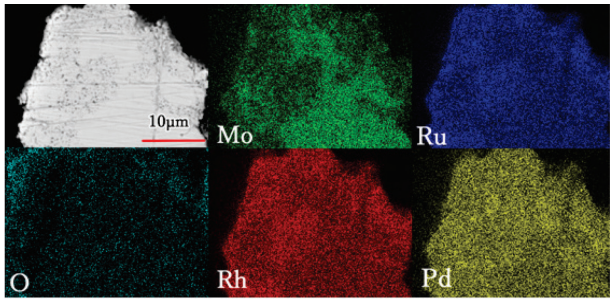

Fig. 9 EDS mapping of R6-3 (P_{O2}=0.01 atm) after heating

Although R6-3 (Mo 21.0 wt.%) had a higher Mo concentration than R6-2 (Mo 15.2 wt.%), EDS mapping (Figs. 7 to 9) showed that low Mo concentration areas were spread widely regardless of the oxygen partial pressure. Especially in R6-3 (P_{O2}=0.2 atm) (Fig. 7), the Mo migration was so pronounced that the Mo rich phase disappeared.

As seen in Tables 2 and **3**, R6-3 (Mo 21.0 wt.%) showed a larger decrease in Mo concentration after heating than R6-2 (Mo 15.2 wt.%), especially in R6-3 (Mo 21.0 wt.%) at high oxygen partial pressure, and the Mo-rich phase disappeared completely. This suggests that in R6-3 (Mo 21.0 wt.%), it is likely that some of the Mo and Ru react with oxygen that had entered the alloy through pores to form oxides, since oxygen in the metal is highly mobile. The extent of these phenomena depends on the Mo concentration.

In addition to this, considering the Gibbs free energy of the constituent elements of noble alloys as shown in the section on thermogravimetric analysis, the oxidation of Mo is prioritized, but in the case of local observations like SEM-EDS, if there is less Mo and more Ru as in R6-2 (Mo 15.2 wt.%), the oxidation of Mo and Ru may be competing with each other[4] This is true for very thin Ru films. This suggests that Ru, whether in a very thin film or in dispersed Ru oxides, may indirectly control Mo oxidation.

The increase or decrease in the thermogravimetric curve is due to the dependence of the oxidation and evaporation behavior of Mo and Ru on oxygen partial pressure and temperature, which is closely related to the geometry of the reaction kinetics, and this will be investigated in combination with information on microstructure in the future.

Table 2 Composition of R6-2 (after heating)

P_{O2} (atm)		Mo (wt.%)	Ru (wt.%)	Rh (wt.%)	Pd (wt.%)	O (wt.%)
Before heating		15.2	55.4	19.1	10.4	-
0.2	Mo rich	11.8	54.6	19.6	8.3	5.7
0.2	Mo poor	8.8	56.7	20.1	8.1	6.3
0.07	Mo rich	10.7	56.8	19.4	8.2	4.9
0.07	Mo poor	8.5	55.4	20.6	9.3	6.1
0.01	*1	8.0	60.5	21.8	3.9	5.7

*1 : Indistinguishable between Mo rich and Mo poor, it is almost Mo rich.

Table 3 Composition of R6-3 (after heating)

P_{O2} (atm)		Mo (wt.%)	Ru (wt.%)	Rh (wt.%)	Pd (wt.%)	O (wt.%)
Before heating		21.0	59.8	13.6	5.7	-
0.2	*2	4.0	66.5	15.4	3.8	10.3
0.05	Mo rich	9.9	65.4	14.9	4.8	5.0
0.05	Mo poor	4.4	69.8	16.3	3.6	5.9
0.01	Mo rich	8.5	67.3	15.9	4.8	3.4
0.01	Mo poor	4.3	63.9	23.6	5.1	3.0

*2 : Indistinguishable between Mo rich and Mo poor, it is almost Mo poor.

The results of XRD and SEM-EDS showed that RuO_2 was formed as a thin film or dispersed on the surface of the noble metal alloy after heating, and that the Mo concentration became low, and the evaporated area became porous after Mo was oxidized. The high and low oxygen partial pressures are related to the degree of Mo oxidation and evaporation, the possibility and degree of Ru oxidation (control of Mo oxidation by Ru), and other factors.

We consider R6-3 (Mo 21.0 wt.%), which showed a weight change that was significantly different from the other two sample compositions in the thermogravimetric analysis. Fig. 10 shows the pseudo ternary phase diagram of Mo-Ru-Rh-Pd at 1173 K. The phase of R6-3 is the HCP phase, while R6-1 and R6-2 are the FCC+HCP phase. Perhaps, the phase state difference between R6-1 an R6-2 (two phases at 1173 K) and R6-3 (one phase at 1173 K) could trigger the rapid weight decrease that occurs for R6-3. However, the whole mechanism cannot be explained without phase information after quench cooling and grain geometry information at high magnification.

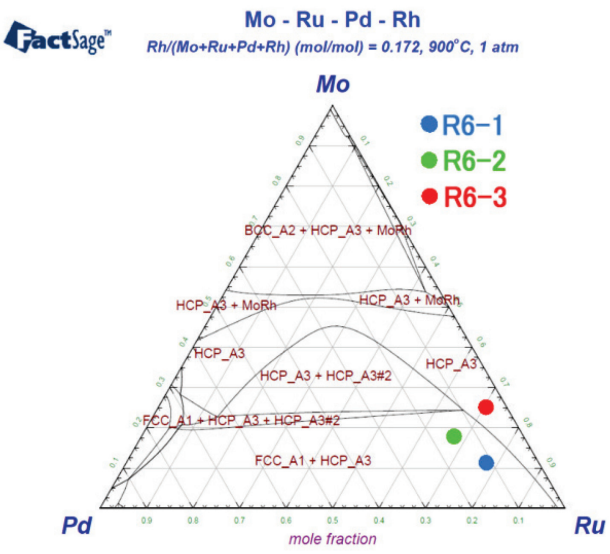

Fig. 10 Mo Ru Pd 3-elements phase diagram (Rh17.2 wt.%) [9].

IV. Conclusion

The dependence of the oxidation and evaporation rates of noble metal alloys on composition and oxygen partial pressure was investigated by changing sample compositions and oxygen partial pressures.

The oxygen partial pressure affects the degree of Mo oxidation and evaporation, the possibility and degree of Ru oxidation (control of Mo oxidation by Ru), and other factors.

Moreover, it can be inferred that there is diversity in the oxidation and evaporation behavior (migration to glass) in the glass melter depending on the location in the melter between the insoluble residue of high burnup fuel or MOX fuel, which is in the FCC+HCP phase, and the insoluble residue of the current fuel, which is in the HCP phase.

However, in this study, the atmosphere was controlled, and only noble metal alloys were subjected to thermogravimetric analysis. It is believed that Mo evaporation rarely occurs in actual glass melters and instead it migrates to the glass side, while Ru and Rh are oxidized at low Mo concentrations [4]. Therefore, TG-DSC analysis of reaction behavior between glass and alloys in the presence of glass with simulated waste liquid components should be conducted to study the behavior of noble metal alloys in environments closer to the actual one.

Acknowledgment

This research is a part of the results of the "FY2023 Basic Research Project on Vitrification Technology for Volume Reduction of Radioactive Waste (JPJ010599)" of the Agency for Natural Resources and Energy, Ministry of Economy, Trade, and Industry, Japan.

References

1) K. Kameyama et al, “Evaluation of undissolved residue characteristics through a burnup analysis of highly burnt LWR fuel,” CRIEPI, Rep. No. T91022 (1992).
2) I. Yamagishi et al, “chemical composition of insoluble residue generated at the Rokkasho reprocessing plant,” *Proc. of Global 2015*, Sep. 20-24, Paris, France, (2015).
3) R. Hattori et al, “Oxidation and vaporization behaviors of insoluble residue (sample) during fabrication of high-level radioactive wastes,” 2020 Fall Meeting of AESJ, Sep. 16-18, (Online Meeting), 2B16, (2020).
4) K. Yamazaki et al, “Oxidation behavior of platinum group alloys in molten glass,” *Electrochemistry*, **92**[4], 043022 (2024).
5) T. Sugawara, T. Ohira, “Estimation of redox condition of simulated high-level waste glass based on the chemical composition of crystalline phases of platinum-group elements,” *Journal of Nuclear Science and Technology*, **15**[1], 43-52 (2016).
6) M. Tanase et al, “Evaluation of a technology for mass production of highly concentrated technetium-99m, solution from molybdenum-99, obtained by the (n, γ) reaction -Fundamental study using non-radioactive rhenium instead of technetium-99m-,” *Radioisotope*, **65**[5], 237-245 (2016).
7) Y. Ohishi et al, “Thermodynamic equilibrium calculations on the oxidation behavior of the Mo-Ru-Rh-Pd alloys,” *Transaction of the AESJ*, **11**[1], 30-36 (2012).
8) National Institute for Materials Science, AtomWork.
9) C. W. Bale et al, Databases: FactPS 8.3, FactSage thermochemical software and databases, 2010 2016” Calphad, 55, 1 19, (2016).